



NJC

A Highly Oxidizing Radical Cation

Journal:	<i>New Journal of Chemistry</i>
Manuscript ID	NJ-ART-09-2020-004434.R1
Article Type:	Paper
Date Submitted by the Author:	06-Oct-2020
Complete List of Authors:	Attanayake, N. Harsha; University of Kentucky, Chemistry; Kaur, Aman Preet; University of Kentucky, Department of Chemistry; University of Kentucky, Department of Materials and Chemical Engineering Suduwella, T. Malsha; University of Kentucky Elliott, Corrine; University of Kentucky, Department of Chemistry Parkin, Sean; University of Kentucky, Chemistry Odom, Susan; University of Kentucky, Chemistry

SCHOLARONE™
Manuscripts

A Stable, Highly Oxidizing Radical Cation

N. Harsha Attanayake,^a Aman Preet Kaur,^a T. Malsha Suduwella,^a Corrine F. Elliott,^a
Sean R. Parkin,^a Susan A. Odom^{*a}

^a Department of Chemistry, University of Kentucky, Lexington, KY 40506, USA

Abstract

Highly oxidizing radical cation salts can be used as chemical oxidants in wide variety of applications. While some are commercial and others can be made, stability has been a problem with many of these organic-based reagents. We sought a method to increase redox potentials of organic compounds, to yield radical cation salts that do not suffer the same instability as their triarylamine counterparts. Using phenothiazines, we (i) blocked the positions *para* to nitrogen with a substituent containing strong covalent bonds, using an electron-withdrawing group to increase oxidation potential, while at the same time (ii) introduced strain at the positions *ortho* to nitrogen to further raise the oxidation potential by preventing geometric relaxation of the oxidized state. Here we synthesized the phenothiazine derivative, *N*-ethyl-1,9-dimethyl-3,7-bis(trifluoromethyl)phenothiazine to test this hypothesis. Indeed, oxidation potentials reflect additive substituent effects, yielding a high-potential redox couple with a stable radical cation. Stability tests in solution and the solid state show that the radical cation form of this phenothiazinium is stable and can be used to oxidize other organic compounds in solution.

Introduction

The introduction of substituents on a redox-active core is a common method used to tailor oxidation and reduction potentials.¹⁻³ The degree of change vs. an original core can often be reliably predicted using Hammett constants, which quantify the degree of electron donation or withdrawal.³⁻⁴ A desire to create high oxidation potential redox couples for electronic and energetic applications has resulted in the synthesis of new materials that contain strongly electron-withdrawing groups.^{1, 5} For example, in developing redox mediators for applications in electrochemical energy storage, our group and others have reported dialkoxybenzene,⁵⁻⁸ TEMPO,⁹⁻¹¹ phenothiazine,¹²⁻¹⁴ and triarylamine derivatives¹⁵⁻¹⁷ that contain electron withdrawing

1
2
3 groups as high potential materials for overcharge protection in lithium-ion batteries (LIBs),
4 polysolutes for redox flow batteries, and redox mediators for lithium-air batteries.
5
6
7

8 While the incorporation of electron-withdrawing groups can be used to reach high oxidation
9 potentials, problems in stability can arise if these redox couples are employed in reducing
10 environments.^{5, 18} Otherwise stable redox couples often decompose if reduced to their radical
11 anion forms.¹⁸⁻¹⁹ For example, dialkoxybenzenes containing phosphonate substituents have
12 oxidation potentials higher than 4 V vs. $\text{Li}^{0/+}$ (this corresponds to about 0.8 V vs.
13 ferrocene/ferrocenium) were designed for overcharge protection of LIBs containing high voltage
14 cathodes. Compared to their lower potential counterparts, their lifetimes in this application were
15 dramatically reduced when employed in electrochemical cells containing highly reducing graphitic
16 anodes.¹⁹⁻²⁰ However, in some cases, less reducing lithium titanate anodes resulted in prolonged
17 lifetimes.²¹ We suspected that reduction to the radical anion form in graphitic anode-containing
18 cells was the cause of the limited lifetimes. Cyclic voltammetry of these derivatives shows that
19 irreversible reduction events are accessible in the electrolyte window, whereas without the
20 electron-withdrawing groups, reduction events were too low in potential to be observed. Our group
21 has observed similar results in the development of high-potential phenothiazine derivatives that
22 oxidize at or above 4 V vs. $\text{Li}^{0/+}$ (ca 0.8 V vs. $\text{Cp}_2\text{Fe}^{0/+}$).^{1, 18} Clearly, a different strategy must be
23 employed for the development of high potential redox couples that exhibit reductive stability.
24
25
26
27
28
29
30
31
32
33
34

35 Apart from the applications in energy storage, the charged forms of stable, high-potential
36 materials are of interest as initiators and as chemical oxidants in organic synthesis.²²⁻²³ The
37 electron-donating, high oxidation potential organic compounds with stable charged states are
38 interesting as organic photoredox catalysts (as powerful oxidants) to perform reductive electron-
39 transfer reactions.²⁴⁻²⁵ However, most of the radical cations found to have very short lifetime in
40 solution phase, which attributes their low-lying excited state energies.²⁵⁻²⁸ The short lifetimes
41 prevent utilizing radical cation as powerful oxidants.²⁵ Thus, developing organic materials with
42 stable charged forms is needed for the growth of the field of metal-free photoredox chemistry.
43 Also, to be useful as a chemical oxidant, the neutral form of the aromatic compound should have
44 a high oxidation potential and its charged species (radical cation) should have a high chemical
45 stability in the solid phase (for storage purposes) as well as in solution phase (to perform redox
46 reactions).²⁹⁻³¹
47
48
49
50
51
52
53
54
55
56
57
58
59
60

1
2
3
4 An alternative method to modulating redox potentials is to vary conjugation in electronic
5 materials.³²⁻³³ This approach has been employed by altering dihedral angles between conjugated
6 pi systems, such as polyphenylenes and polythiophenes, as well as twisting or bending a planar
7 pi system, such as in twistacenes and fullerenes.³⁴⁻³⁶ Often these changes are designed in neutral
8 forms of the redox cores and are retained in their oxidized or reduced states. Recently, we found
9 that a new approach could be used to tune oxidation potentials in a class of molecules called
10 phenothiazines.³⁷ These heterocyclic fused-ring systems exhibit a bent geometry in their neutral
11 form, and planarize upon oxidation. We found that preventing planarization of the oxidized form,
12 without significantly altering the molecular geometry of the neutral form, resulted in an increase
13 in oxidation potential, offering a route to high potential couples without requiring electron
14 withdrawing groups.³⁷ In fact, even the use of electron-donating methyl groups, which usually
15 lower oxidation potentials of conjugated molecules, raise the oxidation potentials of
16 phenothiazines if placed appropriately.
17
18
19
20
21
22
23
24
25

26 Compared to a parent compound, *N*-ethylphenothiazine (EPT, **Figure 1**), a derivative containing
27 methyl groups *para* to nitrogen, *N*-ethyl-3,7-dimethylphenothiazine (3,7-DMeEPT, **Figure 1**) has
28 a lower oxidation potential, which is expected based on the electron-donating nature of methyl
29 substituents. However, when the methyl groups are placed *ortho* to nitrogen, as with *N*-ethyl-1,9-
30 dimethylphenothiazine (1,9-DMeEPT, **Figure 1**), the effect on oxidation potential is not only the
31 opposite but is larger in magnitude. The impact is nearly as significant as the introduction of two
32 trifluoromethyl groups *para* to nitrogen, as with *N*-ethyl-3,7-bis(trifluoromethyl)phenothiazine (3,7-
33 BCF₃EPT, **Figure 1**). Oxidation potentials are provided in **Table 1**.
34
35
36
37
38
39

40 Seeking even higher redox potentials, we wondered whether the effects of electron-withdrawing
41 groups (as in 3,7-BCF₃EPT)³⁸ and sterically hindering groups (as in 1,9-DMeEPT)³⁷ could be
42 combined constructively to achieve this goal. It was unclear, for example, if the electron-
43 withdrawing effect of the trifluoromethyl groups would be disrupted by the sterically hindering
44 groups preventing relaxation, or would the effect be combined? To answer this question, we
45 targeted a new compound, *N*-ethyl-1,9-dimethyl-3,7-bis(trifluoromethyl)phenothiazine (1,9-DMe-
46 3,7-BCF₃EPT, **Figure 1**), incorporating methyl groups at the *ortho* positions for the steric effect
47 and trifluoromethyl groups at the *para* positions to harness their electron-withdrawing effect. Here
48 we report the synthesis and characterization of this new derivative in comparison to the related
49
50
51
52
53
54
55
56
57
58
59
60

compounds shown in **Figure 1**. Here we present the synthesis of this compound and comparisons to related structures, and demonstrate its use as a shelf-stable chemical oxidant.

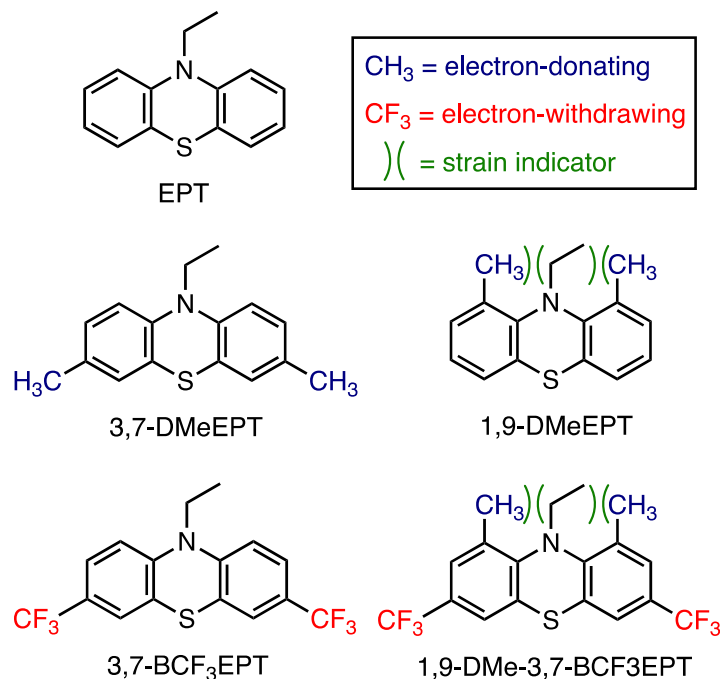
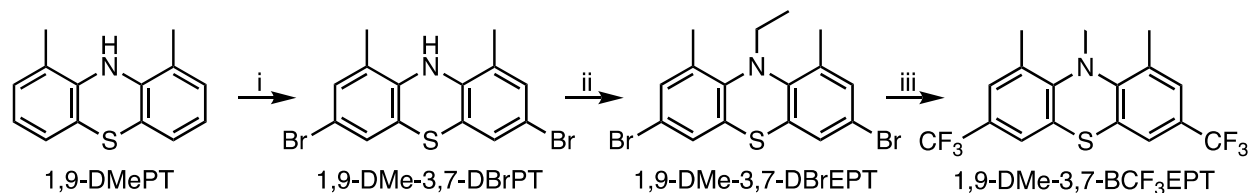


Figure 1. Representations of the chemical structures of *N*-ethylphenothiazine (EPT), *N*-ethyl-3,7-dimethylphenothiazine (3,7-DMeEPT), *N*-ethyl-1,9-dimethylphenothiazine (1,9-DMeEPT), *N*-ethyl-3,7-bis(trifluoromethyl)phenothiazine (3,7-BCF₃EPT), and *N*-ethyl-1,9-dimethyl-3,7-bis(trifluoromethyl)phenothiazine (1,9-DMe-3,7-BCF₃EPT).

Results and Discussion

The synthesis of 1,9-DMe-3,7-BCF₃EPT (**Scheme 1**) was accomplished in three steps starting from 1,9-DMeEPT, which was synthesized following a previously reported procedure for the same compound.³⁷ Bromination of 1,9-DMeEPT produced intermediate 1,9-DMe-3,7-DBrPT, which was then alkylated to obtain 1,9-DMe-3,7-DBrEPT. Finally, 1,9-DMe-3,7-BCF₃EPT was synthesized by treating 1,9-DMe-3,7-DBrEPT with a combination of potassium trifluoroacetate, copper (I) iodide, and cesium fluoride. Synthetic procedures and characterization information are reported in the Experimental Section.



Scheme 1. Synthetic route used to obtain 1,9-DMe-3,7-BCF₃EPT. i. Br₂, CH₃COOH, 24-36 h, r.t. (2.78 g, 51%), ii. a). NaH, DMF/THF, r.t., 30 min, b). CH₃CH₂Br, 80 °C, o/n, (2.15 g, 66%), iii. CF₃CO₂K, CuI, CsF, NMP/DMI, 180 °C, 48 h (0.62 g, 48%).

In addition to standard spectroscopic techniques, X-ray diffraction of single-crystals of 1,9-DMe-3,7-BCF₃EPT (**Figure 2**) provide further support of this product's identity. The thermal ellipsoid plot shows that this derivative is bent through the *N* and *S* atoms, with a butterfly angle (the angle formed by the intersection of the phenyl-ring planes) of 140.5°. This angle is nearly identical to that of 1,9-DMeEPT (146.5°), which does not deviate significantly from derivatives containing *para* substituents, 3,7-DMeEPT (149.3°), and 3,7-BCF₃EPT (144.5-152.1°). All compounds are less bent than the unsubstituted parent EPT (136.8°), (**Table 1, Figure S1**). The main difference in geometries of the 1,9-dimethylated derivatives is expected to be in their radical cation forms. To compare the geometries of radical cations with their neutral forms, we synthesized and isolated the radical cation salts of all EPT derivatives through chemical oxidation with antimony pentachloride (SbCl₅). The radical cation salts had hexachloroantimonate (SbCl₆⁻) as a counter ion. To confirm identity, we grew crystals of radical cation salts conducted analysis using X-ray diffraction. The thermal ellipsoid plots of radical cation salts are shown in **Figure 2** and **Figure S1**. In addition, we compared butterfly angles in these systems to results from density functional theory (DFT), as we know they are a reliable predictor of molecular geometries in this class of molecules. DFT calculations predict the radical cation butterfly angle for 1,9-DMe-3,7-BCF₃EPT to be 156.9°, which is similar to the computed value for the radical cation of 1,9-DMeEPT (156.6°). The isolated single-crystals of 1,9-DMe-3,7-BCF₃EPT and 1,9-DMeEPT radical cations show butterfly angles of 162.8° and 164.9° respectively, confirming that charged forms of strained phenothiazine radical cations remain bent. By contrast, the calculated butterfly angles of the radical cations of unstrained derivatives EPT, 3,7-DMeEPT, and 3,7-BCF₃EPT are significantly more planar; all lie between 171 and 172°, which are close to experimentally obtained values

(174° to 175°). These results suggest that, like 1,9-DMeEPT, the geometric relaxation of the radical cation of 1,9-DMe-3,7-BCF₃EPT will be limited. The experimental and calculated butterfly angles are given in **Table 1** and **Table S2**, respectively. The calculated adiabatic ionization potential (AIP) of 1,9-DMe-3,7-BCF₃EPT is consistent with this trend (**Figure 3**, **Table S1**). In fact, the AIP for 1,9-DMe-3,7-BCF₃EPT (7.22 eV, +0.74 eV vs. EPT at 6.48 eV) is almost the sum of the effect of the substituents on their simpler counterparts, 1,9-DMeEPT (6.68 eV, +0.20 eV vs. EPT) and 3,7-BCF₃EPT (7.06 eV, +0.58 eV vs. EPT). See **Table S1** for AIP values.

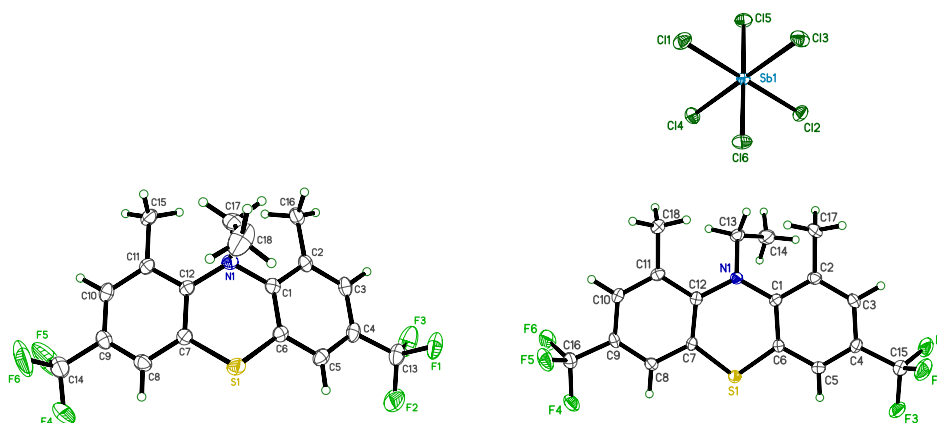


Figure 2. Thermal ellipsoid plot of neutral (left) and radical cation (right) of 1,9-DMe-3,7-BCF₃EPT, obtained by single-crystal X-ray diffraction. The radical cation salts have hexachloroantimonate (SbCl₆⁻) as a counter ion.

Table 1. Comparison of butterfly angles of neutral and radical cation forms of phenothiazine derivatives, obtained from X-ray crystallography. The radical cations salts had hexachloroantimonate (SbCl₆⁻) as the counter ion. Half-wave first oxidation potentials ($E_{1/2}^{0/+}$) vs. Cp₂Fe^{0/+}.

Compound	Butterfly angles [°]		$E_{1/2}^{0/+}$ vs. Cp ₂ Fe ^{0/+} (V)
	neutral	radical cation	
EPT	136.8 ^[a]	174.8 ^[a]	0.27
3,7-DMeEPT	149.3 ^[a]	174.9	0.13
1,9-DMeEPT	146.5 ^[a]	164.9	0.53
3,7-BCF ₃ EPT	144.5-152.1 ^[a,b]	164.5 ^[a,b]	0.61
1,9-DMe-3,7-BCF ₃ EPT	140.5	162.8	0.88

[a] Ref. 37 [b] Multiple molecules in asymmetric unit.

Cyclic voltammetry (CV) was performed to determine the half-wave oxidation potential and chemical reversibility of 1,9-DMe-3,7-BCF₃EPT. This experiment was done in 0.1 M tetrabutylammonium hexafluorophosphate (*n*Bu₄NPF₆) in DCM. A cyclic voltammogram of 1,9-DMe-3,7-BCF₃EPT is shown in **Figure 4a**. It shows a first reversible oxidation and a second irreversible oxidation (**Figure S4**). No reduction event was observed. The first oxidation, at 0.88 V vs. Cp₂Fe^{0/+} at 0 V, is the highest in the series of compounds studied. Compared to EPT ($E_{1/2}^{0/+} = 0.27$ V vs. Cp₂Fe^{0/+}), the oxidation potential of 1,9-DMeEPT ($E_{1/2}^{0/+} = 0.53$ V vs. Cp₂Fe^{0/+}) is 0.26 V higher, and that of 3,7-BCF₃EPT ($E_{1/2}^{0/+} = 0.61$ V vs. Cp₂Fe^{0/+}) is 0.34 V higher. The oxidation potential of 1,9-DMe-3,7-BCF₃EPT is nearly identical to what would be predicted by simply combining the effects of the *ortho* methyl substituents and *para* trifluoromethyl substituents (0.87 V vs. Cp₂Fe^{0/+}), supporting the proposition that the effect of the substituents is indeed additive. These values are in good agreement with the calculated AIPs, as shown in a plot of AIP vs. $E_{1/2}^{0/+}$ (**Figure 3**), for which a line of best fit has an R² value of 0.94.

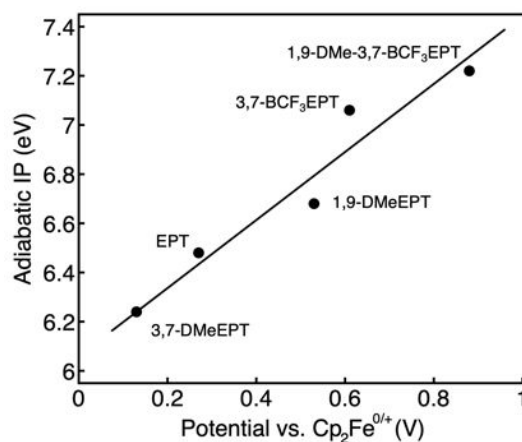


Figure 3. Plot of calculated AIPs vs. half-wave oxidation potentials. The equation for the line of best fit, $y = 0.7039x - 4.257$, has an R² value of 0.94.

The first oxidation is chemically reversible in this electrolyte, as evidenced by the ratio of forward to reverse current (I_{pa}/I_{pc}) of 1.05 (**Table S1**). Variable scan rate voltammograms (**Figure 4b** and **Figure S5**) were performed to determine values of the diffusion coefficients of the neutral and radical cations, determined from Randles-Sevcik plots (**Figure 4c** and **Figure S5**). The diffusion coefficient for neutral 3,7-DMeEPT, 3,7-BCF₃EPT, and 1,9-DMe-3,7-BCF₃EPT are nearly the same, and are all slower than derivatives without *para* substituents. However, the case of the

radical cations is more variable, with rates increasing as follows: 1,9-DMe-3,7-BCF₃EPT < 3,7-DMeEPT < 3,7-BCF₃EPT < 1,9-DMeEPT < EPT. While the derivatives without *para* substituents again have the highest diffusion coefficients, the substituent positions are not enough to explain the trend. Perhaps two trends are competing, such as molecular shape and charge distribution, both of which could affect the solvation spheres.

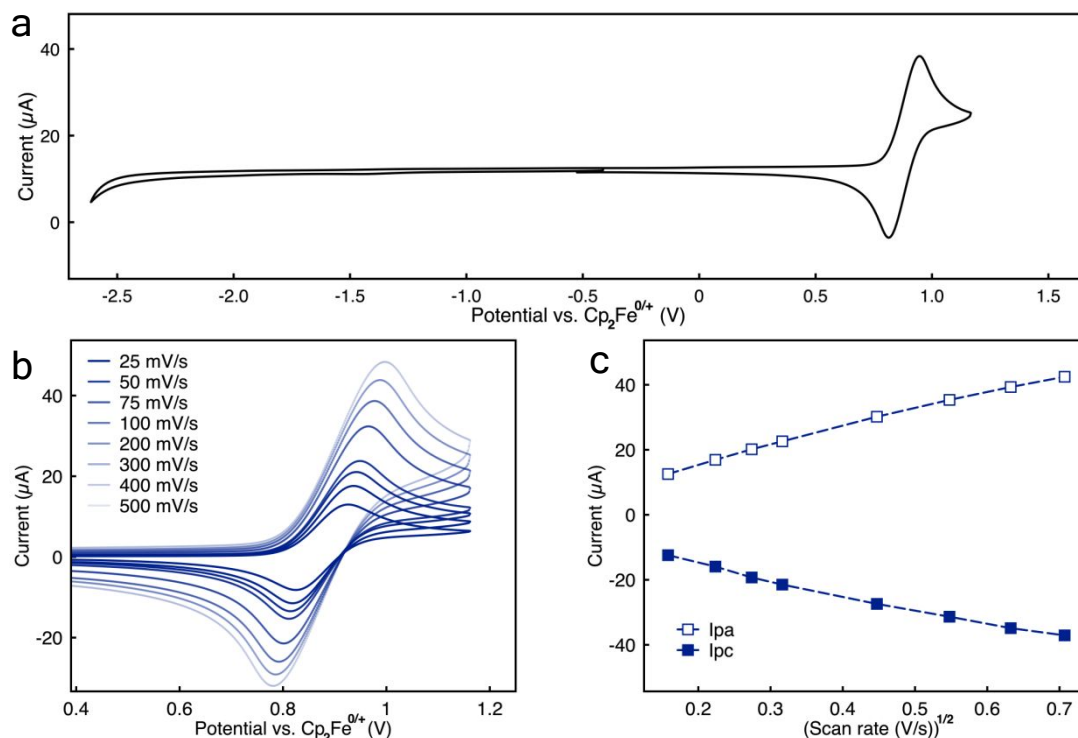


Figure 4. Cyclic voltammogram of 1,9-DMe-3,7-BCF₃EPT at 1 mM in 0.1 M nBu₄NPF₆/DCM, recorded at a scan rate of 100 mV/s (a). The potential is calibrated to $\text{Cp}_2\text{Fe}^{0/+}$ at 0 V, using ferrocene as an internal reference. The scan-rate dependent cyclic voltammograms of the first oxidation event of 1,9-DMe-3,7-BCF₃EPT at 1 mM in 0.1 M nBu₄NPF₆ in DCM, recorded at scan rates ranging from 25 to 500 mV/s (b). Plot of peak current vs. the square root of the scan rate (c).

Given that the first oxidation event was reversible on the CV time scale, at scan rates 25 mV/s, we wanted to further evaluate the stability of the radical cation form of 1,9-DMe-3,7-BCF₃EPT, as radical cations are generally the more reactive form of a neutral/radical cation couple. For this purpose, we utilized the chemically synthesized and isolated radical cation salts of all EPT derivatives to examine the stability of the charged species. The thermal ellipsoid plots of isolated

1
2
3
4 crystals of the radical cation salts are shown in **Figure S1**. The isolation of X-ray quality crystals
5 of radical cations confirms the substantial stability of charged forms, especially, 1,9-dimethylated
6 strained phenothiazine derivatives. To further evaluate the chemical stability of radical cation
7 forms in solution phase, we analyzed samples using UV-vis spectroscopy. We began with a
8 solution of radical cation salts in 0.2 mM concentration in anhydrous DCM using 10 mm path
9 length cuvettes (**Figure 5**). The absorption spectra of the neutral compounds (**Figure S6**) do not
10 overlap with the regions of interest for the radical cations (**Figure 5a**), where distinctive features
11 are observed. In the neutral forms, the absorption spectra of the derivatives containing *ortho*
12 substituents to N are blue shifted compared those that do not. Likewise, differences in the radical
13 cation spectra are observed based on whether compounds contained *ortho* substituents.
14 Specifically, the unstrained compounds exhibit features in close proximity and intensity in the
15 region from 400-600 nm. However, the radical cations of strained 1,9-DMeEPT and 1,9-DMe-3,7-
16 BCF₃EPT lack the finer structure in the lower energy region and instead show a broad absorption,
17 and each exhibits a similarly shaped, more intense absorption feature between 500 and 600 nm
18 that lacks the definition observed in the unstrained equivalents (**Figure 5a and Figure S6**).
19
20
21
22
23
24
25
26
27
28
29
30
31
32
33
34
35
36
37
38
39
40
41
42
43
44
45
46
47
48
49
50
51
52
53
54
55
56
57
58
59
60

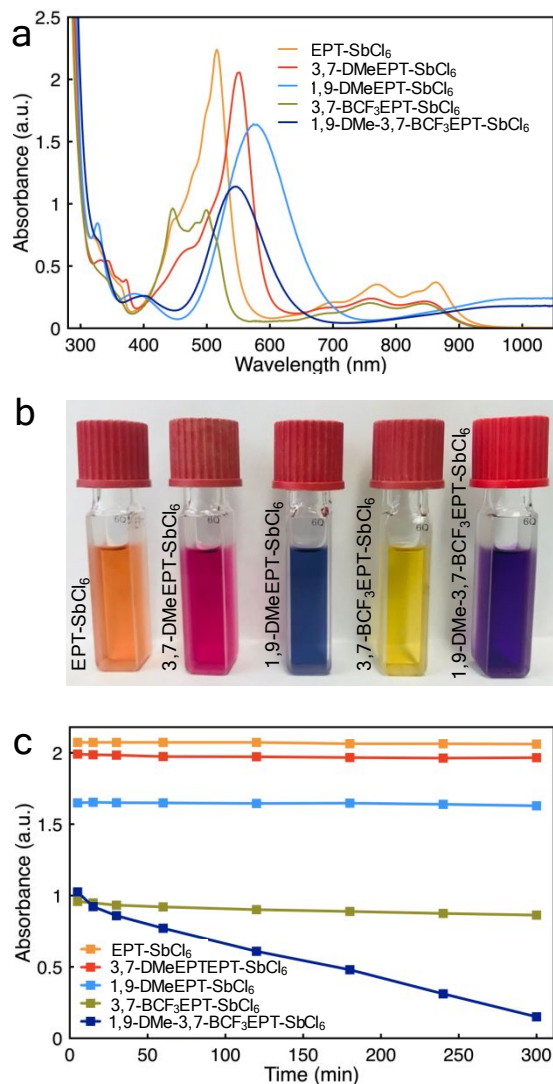


Figure 5. UV-vis absorption spectra of EPT, 3,7-DMeEPT, 1,9-DMeEPT, 3,7-BCF₃EPT and 1,9-DMe-3,7-BCF₃EPT in their radical cation form at 0.20 mM (a), a photograph of cuvettes containing solutions of the radical cations dissolved in DCM and filled in 10 mm path length cuvettes (b), and a plot of absorbance vs. time for radical cations in DCM, collected at 5,15, 30, 60, 120, 180, 240, and 300 min (c). The absorption intensity was monitored at absorption maxima of each radical cation (provided in Table S1). The radical cation salts had hexachloroantimonate (SbCl₆⁻) as a counter ion. UV-vis absorption spectra were recorded using 10 mm path length quartz cuvettes.

We monitored the shape and intensity changes of radical cation absorption spectra for 5 h after dissolving the isolated salts in anhydrous DCM at 0.2 mM (Figure S7). Plotted in Figure 5c are the values for absorption intensity at maximum absorbance vs. time. For the unstrained derivatives as well as strained 1,9-DMeEPT, negligible loss in intensity was observed. However,

1
2
3 for strained 1,9-DMe-3,7-BCF₃EPT, the intensity decreased by *ca.* two thirds over 5 h. Notably,
4 in all cases, the shapes of the absorption spectra remained similar regardless of retention or loss
5 in intensity (**Figures S7a-e**). We pondered the reason for the decay in absorbance intensity for
6 1,9-DMe-3,7-BCF₃EPT. No precipitate was observed in the cuvette, which led us to conclude that
7 the compound was either being transformed into a new species via covalent bond
8 cleavage/formation or underwent an electron-transfer reaction/self-discharge with the solvent and
9 returned to its neutral form.
10
11
12
13
14
15

16 To determine whether the radical cation decomposed and/or underwent electron transfer more
17 rapidly the low (0.2 mM) concentration employed due to trace impurities present in the solvent,
18 we performed another UV-vis experiment at three elevated concentrations. **Figures 6a-c** show the
19 absorption spectra vs. time for three concentrations of radical cation form of 1,9-DMe-3,7-
20 BCF₃EPT at 1, 5, and 10 mM in anhydrous DCM. We analyzed the radical cation salt at these
21 elevated concentrations by using a shorter path length cuvette (2 mm) and by accepting that the
22 absorption spectra of the 5 and 1 mM solution would saturate the detector at the most intense
23 absorption region of radical cation (450-650 nm). Therefore, we monitored the absorption intensity
24 changes in the low energy region (951 nm) for all concentrations. If it is true that trace impurities
25 are responsible for an electron-transfer reaction that causes the radical cation of 1,9-DMe-3,7-
26 BCF₃EPT to transform into its neutral form more rapidly at lower concentrations, and if impurities
27 are acting as reagents rather than catalysts, then at a sufficiently high concentration, the rate of
28 radical cation loss over time should be much lower.³⁹ As shown in **Figure 6d**, radical cations
29 decayed at a faster rate during the first hour compared to rest of 4 hours, which might indicate
30 that radical cations react with most of the trace solvent impurities just after dissolution. It appears
31 that (**Figure 6d**) radical cations are more persistent in the solution when moving from 1 mM to 10
32 mM concentration and the rate of decay is inversely proportional to the concentration. This result
33 offers promise for higher stability and less material decomposition at elevated concentrations in
34 solution phase, as we speculated.
35
36
37
38
39
40
41
42
43
44
45
46
47
48
49
50
51
52
53
54
55
56
57
58
59
60

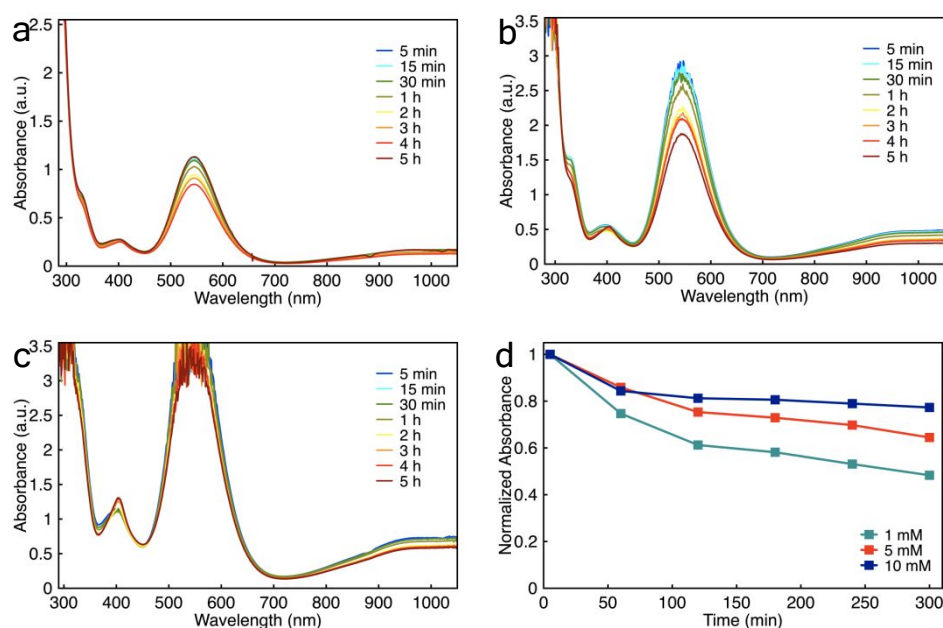


Figure 6. UV-vis absorption spectra of 1,9-DMe-3,7-BCF₃EPT-SbCl₆ radical cation salts at 1 mM (a), 5 mM (b), 10 mM (c), in DCM, and a plot of normalized absorbance (at 951 nm) vs. time for radical cations at each concentration (d), collected at 5, 15, 30, 60, 120, 180, 240, and 300 min. UV-vis absorption spectra were recorded using 2 mm path length quartz cuvettes.

As the radical cation form of 1,9-DMe-3,7-BCF₃EPT shows a significant chemical stability at a higher concentration (10 mM) in solution, we sought to analyze the radical cation stability in the solid state to evaluate this material as a stable chemical oxidant. In general, radical cations can be generated using a few different techniques including bulk electrolysis, irradiation with gamma rays, and reaction with a chemical oxidant.^{29, 40-41} Of these methods, chemical oxidants is quite simple. The chemical radical cation generation process is an electron transfer reaction where the oxidant accepts an electron from the neutral compound, thereby generating the radical cation form. For a compound to serve as a chemical oxidant, it is necessary that the oxidation potential of neutral form of the chemical oxidant be than the neutral form of molecule to be oxidized. As 1,9-DMe-3,7-BCF₃EPT shows the highest oxidation potential ($E_{1/2}^{0/+} = 0.88$ V vs. Cp₂Fe^{0/+}) among molecules in this study, its radical cation form should be able to chemically oxidize all phenothiazine derivatives, ranging from the lowest oxidation potential 3,7-DMeEPT ($E_{1/2}^{0/+} = 0.13$ V vs. Cp₂Fe^{0/+}) to the next highest oxidation potential 3,7-BCF₃EPT ($E_{1/2}^{0/+} = 0.61$ V vs. Cp₂Fe^{0/+}).

For this purpose, 1,9-DMe-3,7-BCF₃EPT-SbCl₆ was freshly synthesized and stored under two different conditions to examine its shelf life stability in the solid state for three weeks: (i) stored in a glass vial inside an argon filled glove box, and (ii) stored in a glass vial on the bench top. In addition to the radical cations of 1,9-DMe-3,7-BCF₃EPT, we analyzed the shelf life stability of freshly synthesized EPT-SbCl₆ as a control. As shown in **Figure 7** (1,9-DMe-3,7-BCF₃EPT-SbCl₆) and **Figure S8** (EPT-SbCl₆), the UV-vis spectra of radical cation samples were recorded on days 0, 7, 14, and 21 after freshly preparing radical cation solutions in anhydrous DCM. We analyzed 1,9-DMe-3,7-BCF₃EPT radical cation at 1 mM in 2 mm pathlength cuvettes.

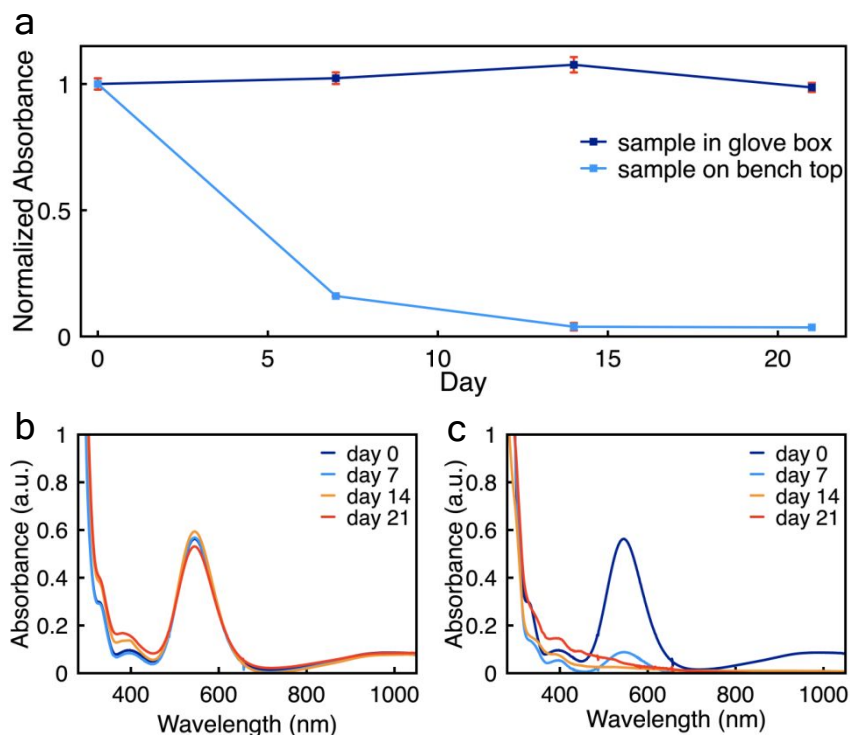


Figure 7. Solid state stability of 1,9-DMe-3,7-BCF₃EPT-SbCl₆ on day 0, 7, 14, and 21 following storage in glass vials, placed in an argon filled glove box in light and on a bench top in light. Normalized absorbance intensity at 545 nm vs. time for 1,9-DMe-3,7-BCF₃EPT-SbCl₆ (a). UV-vis absorption spectra of 1,9-DMe-3,7-BCF₃EPT-SbCl₆, stored in an argon filled glove box (b), on the bench top (c) at 1 mM in DCM. UV-vis absorption spectra were recorded using 2 mm path length quartz cuvettes.

EPT-SbCl₆ stored in the glove box and on the benchtop remained stable over three weeks without showing new peaks or without losing absorption intensity on UV-vis spectra (**Figures S8b and**

1
2
3
4 **S8c**). The plot of normalized absorbance intensity at maximum absorbance vs. time of the EPT
5 radical cation (**Figure S8a**) shows, it is stable in solid state for three weeks, regardless of the
6 exclusion of water and oxygen or not. 1,9-DMe-3,7-BCF₃EPT-SbCl₆ showed environment-
7 dependent stability. Although, the sample stored in the glove box remained similarly stable to
8 EPT-SbCl₆ (**Figures 7a and 7b**), the one kept on the benchtop decomposed significantly in the
9 solid state (**Figures 7a and 7c**). The loss of absorbance intensity is evident in the spectrum shown
10 in **Figure 7c**; the change in spectral shape indicates that 1,9-DMe-3,7-BCF₃EPT-SbCl₆ is sensitive
11 to atmospheric moisture and/or air. However, its stability is greater than that of Magic Blue (MB,
12 tris(4-bromophenylammonium)hexachloroantimonate), a commercially available chemical oxidant
13 that has been employed as a one-electron oxidant in various fields,⁴²⁻⁴³ is also known that to
14 decompose in the solid state – even upon storage in an inert atmosphere, generating byproducts
15 called the “blues brothers”, by dimerizing through its labile C-Br bonds.⁴⁴⁻⁴⁵ This not only prevents
16 the accuracy of the quantitative analysis of the oxidation process, but also may mislead the
17 spectroscopic analysis. However, 1,9-DMe-3,7-BCF₃EPT-SbCl₆ is at least as stable in an inert
18 environment in the solid state, perhaps due to its strong covalent bonds. We suspect that 1,9-
19 DMe-3,7-BCF₃EPT-SbCl₆ decomposed in ambient conditions due to the formation of S=O or SO₂
20 compounds by reacting with atmospheric oxygen/ water.
21
22
23
24
25
26
27
28
29
30
31
32
33

34 **Conclusions**

35 Here we showed that the combination of electron-donating groups positioned at locations that
36 prevent the relaxation of the radical cation form, in combination with electron-withdrawing groups
37 at unstrained positions, have an additive effect on the oxidation potential of phenothiazines
38 compared to derivatives having only one type of substituent. The oxidation potential of both
39 strained and electron-withdrawing substituents resulted in the creation of a new high-potential
40 redox couple with different electronic structure compared to its unstrained counterparts. The first
41 oxidation event of the neutral compound is reversible by cyclic voltammetry at scan rates from 25
42 to 500 mV/s. Importantly, the introduction of substituents to create this high-potential couple did
43 not bring the reduction event into the solvent window. This result highlights a key advantage of
44 this approach over introduction of more electron-withdrawing groups to raise oxidation potentials,
45 which – if sufficiently electron-withdrawing – bring the first reduction event, which is irreversible,
46 into the solvent window. This feature may allow for strained phenothiazines to be used in
47
48
49
50
51
52
53
54
55
56
57
58
59
60

1
2
3 applications that involve highly reducing environments and for their radical cation to be used as a
4 strong oxidizing agent with stability greater than other organic oxidants.
5
6

7 8 **Experimental Section**

9 10 11 **I. General**

12 Potassium trifluoroacetate, copper (I) iodide, and cesium fluoride were purchased from Sigma
13 Aldrich. Sodium hydride (60% dispersion in mineral oil), magnesium sulfate, *N*-methylpyrrolidone
14 (NMP), 1,3-dimethyl-2-imidazolidinone (DMI), sodium sulfite, potassium hydroxide and antimony
15 pentachloride (SbCl₅) were purchased from Acros Organics. Bromine, acetic acid, and
16 tetrabutylammonium hexafluorophosphate (*n*Bu₄NPF₆) were purchased from Sigma Aldrich.
17 Anhydrous dichloromethane (DCM), anhydrous tetrahydrofuran (THF), and anhydrous *N,N*-
18 dimethylformamide (DMF) were purchased from VWR and stored in a solvent purification system
19 (L.T. Technologies). Silica gel used for column chromatography was purchased from Sorbent
20 Technologies. Ethyl acetate and hexanes for column chromatography were purchased from
21 Avantor Performance Materials. Solvents used for NMR spectroscopy were obtained from
22 Cambridge Isotope Laboratories. ¹H, ¹⁹F and ¹³C NMR spectra were obtained on a 400 MHz
23 Varian NMR spectrometer. ¹⁹F NMR, chemical shifts are reported vs. CFC₃ at 0 ppm by adjusting
24 the chemical shift of hexafluorobenzene (Alfa Aesar), used as an internal reference, to -164.9
25 ppm. Mass spectra were obtained on an Agilent 5973 Network mass selective detector attached
26 to Agilent 6890N Network GC system. Elemental analyses were performed by Atlantic Microlab,
27 Inc.
28
29
30
31
32
33
34
35
36
37
38
39

40 **II. Synthesis**

41 *N*-Ethylphenothiazine (EPT),⁴⁶ *N*-ethyl-3,7-dimethylphenothiazine (3,7-DMeEPT),⁴⁷ *N*-ethyl-3,7-
42 bis(trifluoromethyl)phenothiazine (BCF₃EPT),³⁸ bis(*o*-tolyl)amine, 1,9-dimethylphenothiazine
43 (1,9-DMePT), *N*-ethyl-1,9-dimethylphenothiazine (1,9-DMeEPT),³⁷ and *N*-ethylphenothiazine-
44 hexachloroantimonate (EPT-SbCl₆),²⁹ were synthesized as previously reported.
45
46
47
48
49

50 **3,7-Dibromo-1,9-dimethylphenothiazine (1,9-DMe-3,7-DBrPT).** In an oven-dried 250 mL round-
51 bottomed flask under nitrogen atmosphere, 1,9-DMePT (3.25 g, 14.3 mmol) was dissolved in
52 anhydrous acetic acid (100 mL). A solution of bromine (2.12 mL, 41.5 mmol) in acetic acid (15
53 mL) was slowly transferred into the reaction mixture using an addition funnel. Then the reaction
54
55
56
57
58
59
60

1
2
3
4 mixture was stirred in room temperature for a day until consumption of starting materials. Sodium
5 sulfite (1.22 g, 2.02 mmol) was added into reaction mixture and stirred for 2 h till get a gray
6 solution. After that reaction mixture was transferred into a 1 L beaker. Potassium hydroxide (2.51
7 g, 42.9 mmol) was dissolved in deionized water (100 mL) and the volume was raised to 300 mL
8 after adding ice. This solution was poured into the reaction mixture and stirred using a glass rod,
9 yielding a gray precipitate, which was filtered, rinsed with more deionized water, then dried
10 overnight in a vacuum oven (50 °C, -0.1 MPa). Finally, the solid product was crystallized from
11 ethanol, yielding the product as a gray crystalline solid (2.78 g, 51%). ¹H NMR (400 MHz, DMSO-
12 *d*₆) δ 7.18 (m, 2H), 7.09 (m, 2H), 6.85 (s, 1H), 2.25 (s, 6H). ¹³C NMR (100 MHz, CDCl₃) δ 138.9,
13 133.3, 133.0, 131.7, 127.2, 114.3, 16.8. GCMS: *m/z* 385 (100%), 383 (91%), 304 (37%), 302
14 (34%), 224 (38%), 192 (12%), 180 (8%), 111(10%). Anal. Calcd. for C₁₄H₁₁Br₂NS: C, 43.66; H,
15 2.88; N, 3.64. Found C, 43.85; H, 2.97; N, 3.63.
16
17
18
19
20
21
22
23

24 **3,7-Dibromo-N-ethyl-1,9-dimethylphenothiazine (1,9-DMe-3,7-DBrEPT).** In an oven-dried 250 mL
25 round-bottomed flask under nitrogen atmosphere, 1,9-DMe-3,7-DBrPT (3.00 g, 7.80 mmol) was
26 dissolved in a solution of anhydrous DMF (60 mL) and anhydrous THF (60 mL). Sodium hydride
27 (0.78 g, 60 wt.% in mineral oil, 20 mmol) was added at room temperature, and the reaction mixture
28 was stirred for 30 min. After that bromoethane (1.02 g, 48.6 mmol) was added to the reaction
29 mixture and round bottom flask was equipped with a reflux condenser. Then the reaction mixture
30 was refluxed by heating in an oil bath at 90 °C for 12 h. After completion the reaction, reaction
31 mixture was cooled to room temperature and quenched with water. The organic product was
32 extracted with ethyl acetate, and it was washed with brine and dried over MgSO₄. The organic
33 extracts were filtered and concentrated by rotary evaporation. The resulting organic crude was
34 purified by silica gel column chromatography using a gradient of 0–4% ethyl acetate in hexanes
35 as eluent, yielding the product as a white solid (2.15 g, 66%). ¹H NMR (400 MHz, DMSO-*d*₆) δ
36 7.41 – 7.31 (m, 4H), 3.39 (q, *J* = 7.0, 2H), 2.34 (s, 6H), 0.95 (t, *J* = 7.1, 3H). ¹³C NMR (100 MHz,
37 CDCl₃) δ 142.9, 135.9, 135.8, 132.2, 127.1, 117.4, 49.6, 18.2, 14.1. GCMS: *m/z* 413 (23%), 384
38 (100%), 382(54%), 304 (8%), 223 (10%). Anal. Calcd. for C₁₆H₁₅Br₂NS: C, 46.51; H, 3.66; N, 3.39.
39 Found C, 46.59; H, 3.82; N, 3.34.
40
41
42
43
44
45
46
47
48
49
50

51 **N-Ethyl-1,9-dimethyl-3,7-bis(trifluoromethyl)phenothiazine (1,9-DMe-3,7-BCF₃EPT).** 1,9-DMe-
52 3,7-DBrEPT (1.25 g, 3.03 mmol) and copper(I) iodide (4.61 g, 24.2 mmol) were added into an
53 oven dried 100 mL pressure vessel under nitrogen atmosphere. The pressure vessel was
54
55
56
57
58
59
60

1
2
3 transferred to an argon filled glove box, then potassium trifluoroacetate (2.76 g, 18.2 mmol) and
4 cesium fluoride (0.99 g 6.5 mmol) were added into the pressure vessel and removed from the
5 glove box. *N*-Methylpyrrolidinone (NMP) (44 mL) and 1,3-dimethyl-2-imidazolidinone (10 mL)
6 were added under N₂ atmosphere to the reaction mixture, which was sparged with N₂ for 10 min
7 while immersed in oil bath preheated to 90 °C. The pressure vessel was sealed, and the
8 temperature of the oil bath was raised to 180 °C after which the reaction mixture was stirred for
9 48 h. The reaction flask was removed from the oil bath, and the reaction mixture was allowed to
10 cool to room temperature, then diluted with ethyl acetate and filtered through a pad of celite. Water
11 was added to the filtrate and organic product was extracted with ethyl acetate. The combined
12 organic layers were washed with brine and dried over MgSO₄. The organic extracts were filtered
13 and concentrated by rotary evaporation. The resulting organic crude was purified by silica gel
14 column chromatography using a gradient of 0-2% ethyl acetate in hexanes as the eluent, yielding
15 the product as a white crystalline solid (0.62 g, 48%). ¹H NMR (400 MHz, DMSO-*d*₆) δ 7.58 – 7.51
16 (m, 4H), 3.57 (q, *J* = 7.1 Hz, 2H), 2.43 (s, 6H), 0.99 (t, *J* = 7.1 Hz, 3H). ¹³C NMR (100 MHz, CDCl₃)
17 δ 147.1, 134.9, 134.5, 127.0, 125.5, 122.8, 122.1, 50.1, 18.9, 14.8. ¹⁹F NMR (400 MHz, CDCl₃) δ
18 -65.4 (s, 6F). GCMS: *m/z* 391 (23%), 362 (100%), 330 (8%). Anal. Calcd. for C₁₈H₁₅F₆NS: C,
19 55.24; H, 3.86; N, 3.58. Found C, 55.04; H, 4.05; N, 3.60.
20
21
22
23
24
25
26
27
28
29
30
31

32 ***N*-Ethyl-3,7-dimethylphenothiazine hexachloroantimonate (3,7-DMeEPT-SbCl₆).** 3,7-DMeEPT
33 (0.10 g, 0.39 mmol) was dissolved in anhydrous dichloromethane (5 mL) in an oven-dried 25 mL
34 round-bottomed flask fitted with a rubber septum under nitrogen atmosphere after which the
35 round-bottomed flask immersed in an ice water bath for 10 min. Then antimony pentachloride
36 (0.080 mL, 0.58 mmol) was added into reaction mixture and stirred 15 min. Upon completion of
37 the reaction, anhydrous diethyl ether (15 mL) was added gradually with continued stirring,
38 resulting in a dark pink precipitate. The precipitate was filtered under nitrogen, then washed with
39 more diethyl ether (20-30 mL) to remove unreacted starting material. The solid dark pink product
40 (0.11 g, 50%) was dried under nitrogen and stored in a glove box. To grow crystals of this product,
41 a saturated solution of 3,7-DMeEPT-SbCl₆ salt in anhydrous DCM was prepared. Then, a small
42 volume of saturated solution (0.5 mL) transferred in an NMR tube and slowly layered it with
43 anhydrous toluene (0.5 mL) to form two layers. Finally, the NMR tube was capped and vertically
44 placed in a freezer set at 4 °C, and crystals formed at the interface of the solvents.
45
46
47
48
49
50
51
52
53
54
55
56
57
58
59
60

1
2
3
4 ***N*-Ethyl-1,9-dimethylphenothiazine hexachloroantimonate (1,9-DMeEPT-SbCl₆)**. 1,9-DMeEPT
5 (0.10 g, 0.39 mmol) was dissolved in anhydrous dichloromethane (5 mL) in an oven-dried 25 mL
6 round-bottomed flask fitted with a rubber septum under nitrogen atmosphere, then round-
7 bottomed flask was cooled in an ice water bath for 10 minutes. Then antimony pentachloride
8 (0.080 mL, 0.58 mmol) was added into reaction mixture and stirred 15 minutes. Upon completion
9 of the reaction, anhydrous diethyl ether (15 mL) was added gradually with continued stirring,
10 resulting in a blue precipitate. The precipitate was filtered under nitrogen, then washed with more
11 diethyl ether (20-30 mL) to remove unreacted starting material. The solid blue product (0.10 g,
12 43%) was dried under nitrogen and stored in a glove box. To grow crystals of this product, a
13 saturated solution of 1,9-DMeEPT-SbCl₆ salt in anhydrous DCM was prepared. Then, a small
14 volume of saturated solution (0.5 mL) transferred in an NMR tube and slowly layered it with
15 anhydrous diethyl ether (0.5 mL) to form two layers. Finally, the NMR tube was capped and
16 vertically placed in a freezer set at 4 °C, and crystals formed at the interface of the solvents.
17
18
19
20
21
22
23
24
25

26 ***N*-Ethyl-3,7-bis(trifluoromethyl)phenothiazine hexachloroantimonate (3,7-BCF₃EPT-SbCl₆)**. 3,7-
27 BCF₃EPT (0.10 g, 0.28 mmol) was dissolved in anhydrous dichloromethane (5 mL) in an oven-
28 dried 25 mL round-bottomed flask fitted with a rubber septum under nitrogen atmosphere, then
29 round-bottomed flask was cooled in an ice water bath for 10 minutes. Antimony pentachloride
30 (0.050 mL, 0.41 mmol) was added into reaction mixture and stirred 15 minutes. Upon completion
31 of the reaction, anhydrous diethyl ether (15 mL) was added gradually with continued stirring,
32 resulting in a dark green precipitate. The precipitate was filtered under nitrogen, then washed with
33 more diethyl ether (20-30 mL) to remove unreacted starting material. The solid dark green product
34 (0.12 g, 66%) was dried under nitrogen and stored in a glove box.
35
36
37
38
39
40
41

42 ***N*-Ethyl-1,9-dimethyl-3,7-bis(trifluoromethyl)phenothiazine hexachloroantimonate (1,9-DMe-3,7-
43 BCF₃EPT-SbCl₆)**. 1,9-DMe-3,7-BCF₃EPT (0.18 g, 0.37 mmol) was dissolved in anhydrous
44 dichloromethane (5 mL) in an oven-dried 25 mL round-bottomed flask fitted with a rubber septum
45 under nitrogen atmosphere, then round-bottomed flask was cooled in an ice water bath for 10
46 minutes. Antimony pentachloride (0.080 mL, 0.55 mmol) was added into reaction mixture and
47 stirred 15 minutes. Upon completion of the reaction, anhydrous diethyl ether (15 mL) was added
48 gradually with continued stirring, resulting in a blue precipitate. The precipitate was filtered under
49 nitrogen, then washed with more diethyl ether (20-30 mL) to remove unreacted starting material.
50 The solid purple product (0.14 g, 42%) was dried under nitrogen and stored in a glove box. To
51
52
53
54
55
56
57
58
59
60

1
2
3
4 grow crystals of this product, a saturated solution of 1,9-DMe-3,7-BCF₃EPT-SbCl₆ salt in
5 anhydrous DCM was prepared. Then, a small volume of saturated solution (0.5 mL) transferred
6 in an NMR tube and slowly layered it with anhydrous diethyl ether (0.5 mL) to form two layers.
7 Finally, the NMR tube was capped and vertically placed in a freezer set at 4 °C, and crystals
8 formed at the interface of the solvents.
9

10 11 12 13 **III. X-ray Crystallography**

14 X-ray diffraction data were collected at 180(1) K on a Bruker D8 Venture kappa-axis diffractometer
15 using MoK(alpha) X-rays. Raw data were integrated, scaled, merged and corrected for Lorentz-
16 polarization effects using the APEX3 package.⁴⁸ Corrections for absorption were applied using
17 SADABS.⁴⁹ The structure was solved by direct methods (SHELXT)⁵⁰ and refinement was carried
18 out against F² by weighted full-matrix least-squares (SHELXL).⁵¹ Hydrogen atoms were found in
19 difference maps, but subsequently placed at calculated positions and refined using a riding
20 model. Non-hydrogen atoms were refined with anisotropic displacement parameters. Atomic
21 scattering factors were taken from the International Tables for Crystallography.⁵²
22
23
24
25
26
27
28

29 **V. Computational Studies**

30 All density functional theory (DFT) calculations were performed using the Gaussian09 (Revision
31 A.02b) software suite. Geometry optimizations of the neutral and radical-cation states were
32 carried out using the B3LYP functional at the 6-311G(d,p) level of theory.⁵³ Frequency analyses
33 of all (fully relaxed) optimized geometries were performed to ensure that the geometries were
34 energetic minima. AIP of EPT, 3,7-DMeEPT, 1,9-DMeEPT, and 3,7-BCF₃EPT was taken from ref.
35
36
37
38
39 37.
40
41

42 **IV. Electrochemical Analysis**

43 Cyclic voltammetry (CV) experiments were performed with a CH Instruments 600D potentiostat
44 using a three-electrode system with glassy carbon as the working electrode, freshly anodized
45 Ag/AgCl as the reference electrode, and a Pt wire as the counter electrode at 1 mM analyte in 0.1
46 M nBu₄NPF₆ in DCM. Voltammograms were recorded at a scan rate of 100 mV s⁻¹. Ferrocene or
47 dexamethylferrocene was used as an internal reference and oxidation potentials were calibrated
48 relative to ferrocenium/ferrocene (Cp₂Fe⁺⁰). The diffusion coefficients of the active species at 1
49 mM concentration were calculated using Randles–Sevcik equation,⁵⁴
50
51
52
53
54
55
56
57
58
59
60

$$i_p = 0.4463 nFAc \left(\frac{nFD}{RT} v \right)^{0.5}$$

where i_p is the peak current (A), n is the number of electrons transferred (-), F is the Faraday constant (96485 C mol⁻¹), A is the electrode area (cm²), c is the concentration (mol cm⁻³), D is the diffusion coefficient (cm² s⁻¹), R is the gas constant (8.314 J mol⁻¹ K⁻¹), T is the absolute temperature (K), and v is the scan rate (V s⁻¹). The following scan rates were used for diffusion coefficient calculations: 25, 50, 75, 100, 200, 300, 400, and 500 mV s⁻¹.

VI. UV-vis Spectroscopy

UV-vis spectra were obtained using optical glass cuvettes (Starna) with 2 or 10 mm path length on an Agilent 8453 diode array spectrophotometer. All the radical cation solutions were prepared in anhydrous DCM and transferred into cuvettes inside an argon filled glovebox. The capped cuvettes were taken out from the glove box for spectral analysis.

UV-vis study at 0.2 mM concentration: All phenothiazine radical cation salts (EPT-SbCl₆, 3,7-DMeEPT-SbCl₆, 1,9-DMeEPT-SbCl₆, 3,7-BCF₃EPT-SbCl₆, and 1,9-DMe-3,7-BCF₃EPT-SbCl₆) were dissolved in anhydrous DCM at 0.2 M and pipetted to 1 cm path length cuvettes. UV-vis spectra were collected at 5, 15, 30, 60, 120, 180, 240, 300 min after preparing samples.

UV-vis study at different concentrations: 1,9-DMe-3,7-BCF₃EPT-SbCl₆ was dissolved in anhydrous DCM at 1, 5, and 10 mM and pipetted to 2 mm path length cuvettes. UV-vis spectra were collected at 5, 15, 30, 60, 120, 180, 240, 300 min after preparing samples.

UV-vis study for shelf stability: Freshly synthesized radical cation salts of EPT-SbCl₆ and 1,9-DMe-3,7-BCF₃EPT-SbCl₆ were stored in two different environments; 1. stored in a glass vial and placed inside an argon filled glove box, 2. stored in a glass vial and placed on the bench top. The radical cation salts were weighed either inside of the glove box or outside of the glove box to prepare samples for UV-vis analysis, depending on where it has been stored. Then, all solutions were prepared in anhydrous DCM and transferred into cuvettes inside an argon filled glovebox. EPT-SbCl₆ was analyzed at 0.2 mM (in 10 mm pathlength cuvette) as its solubility is less than 1 mM in DCM and 1,9-DMe-3,7-BCF₃EPT-SbCl₆ was analyzed at 1 mM (in 2 mm pathlength cuvette) as it highly decays at 0.2 mM. At days 0, 7, 14 and 21, required amounts (to make a 0.2

1
2
3 or 1 mM solution) of each radical cation salt stored on bench-top (weighed outside the glovebox)
4 and the ones stored inside the box (weighed inside the glovebox) were dissolved in anhydrous
5 DCM (inside the glovebox) and prepared UV-vis samples for analysis.
6
7
8
9
10
11
12
13
14
15
16
17
18
19
20

21 **Acknowledgements**

22 This work was funded by the National Science Foundation's Division of Chemistry (Award
23 1300653) and EPSCoR Program (Award 1355438). We thank Corrine Elliott and Chad Risko for
24 their computational chemistry efforts. While their results are cited, we could not have done this
25 work without them.
26
27
28
29
30
31
32
33
34

35 **References**

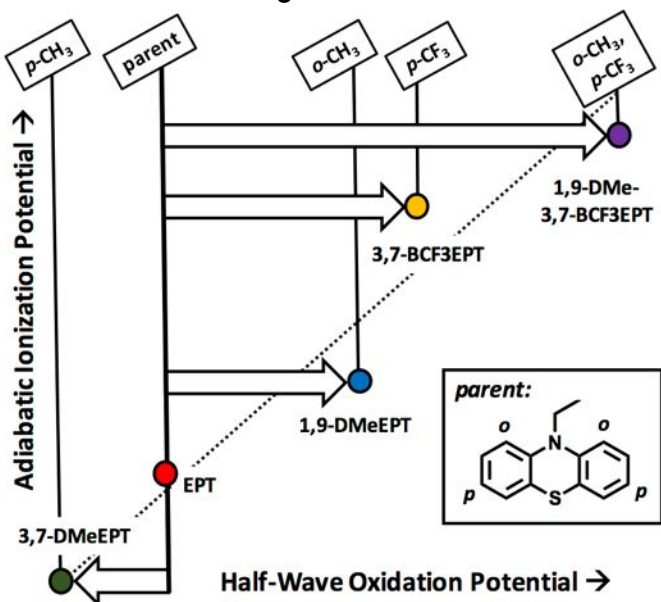
- 36
37
38 1. Ergun, S.; Elliott, C. F.; Kaur, A. P.; Parkin, S. R.; Odom, S. A., Overcharge Performance
39 of 3,7-disubstituted N-Ethylphenothiazine Derivatives in Lithium-ion Batteries. *Chem. Comm.*
40 **2014**, *50*, 5339-5341.
41
42 2. Zhang, J.; Huang, J.; Robertson, L. A.; Shkrob, I. A.; Zhang, L., Comparing Calendar and
43 Cycle Life Stability of Redox Active Organic Molecules for Nonaqueous Redox Flow Batteries.
44 *J. Power Sources* **2018**, *397*, 214-222.
45
46 3. Hammett, L. P., The Effect of Structure Upon the Reactions of Organic Compounds.
47 Benzene Derivatives. *J. Am. Chem. Soc.* **1937**, *59*, 96-103.
48
49 4. Dewar, M. J.; Grisdale, P. J., Substituent Effects. I. Introduction. *J. Am. Chem. Soc.* **1962**,
50 *84*, 3539-3541.
51
52 5. Kowalski, J. A.; Carney, T. J.; Huang, J.; Zhang, L.; Brushett, F. R., An investigation on
53 the impact of halidization on substituted dimethoxybenzenes. *Electrochim. Acta* **2020**, *335*,
54 135580.
55
56 6. Zhang, Z.; Zhang, L.; Schlueter, J. A.; Redfern, P. C.; Curtiss, L.; Amine, K.,
57 Understanding the Redox Shuttle Stability of 3, 5-di-tert-butyl-1, 2-dimethoxybenzene for
58 Overcharge Protection of Lithium-ion Batteries. *J. Power Sources* **2010**, *195*, 4957-4962.
59
60

7. Huang, J.; Su, L.; Kowalski, J. A.; Barton, J. L.; Ferrandon, M.; Burrell, A. K.; Brushett, F. R.; Zhang, L., A Subtractive Approach to Molecular Engineering of Dimethoxybenzene-Based Redox Materials for Non-aqueous Flow Batteries. *J. Mater. Chem. A* **2015**, *3*, 14971-14976.
8. Schwager, P.; Bülter, H.; Plettenberg, I.; Wittstock, G., Review of Local In Situ Probing Techniques for the Interfaces of Lithium-Ion and Lithium–Oxygen Batteries. *Energy Technol.* **2016**, *4*, 1472-1485.
9. Moshurchak, L.; Buhrmester, C.; Wang, R.; Dahn, J., Comparative Studies of Three Redox Shuttle Molecule Classes for Overcharge Protection of LiFePO₄-Based Li-ion Cells. *Electrochim. Acta* **2007**, *52*, 3779-3784.
10. Wei, X.; Xu, W.; Vijayakumar, M.; Cosimbescu, L.; Liu, T.; Sprenkle, V.; Wang, W., TEMPO-Based Catholyte for High-Energy Density Nonaqueous Redox Flow Batteries. *Adv. Mater.* **2014**, *26*, 7649-7653.
11. Bergner, B. J.; Schürmann, A.; Peppler, K.; Garsuch, A.; Janek, J. r., TEMPO: A Mobile Catalyst for Rechargeable Li-O₂ Batteries. *J. Am. Chem. Soc.* **2014**, *136*, 15054-15064.
12. Attanayake, N. H.; Kowalski, J. A.; Greco, K. V.; Casselman, M. D.; Milshtein, J. D.; Chapman, S. J.; Parkin, S. R.; Brushett, F. R.; Odom, S. A., Tailoring Two-Electron-Donating Phenothiazines To Enable High-Concentration Redox Electrolytes for Use in Nonaqueous Redox Flow Batteries. *Chem. Mater.* **2019**, *31*, 4353-4363.
13. Kaur, A. P.; Ergun, S.; Elliott, C. F.; Odom, S. A., 3,7-Bis(trifluoromethyl)-N-ethylphenothiazine: A Redox Shuttle with Extensive Overcharge Protection in Lithium-ion Batteries. *J. Mater. Chem. A* **2014**, *2*, 18190-18193.
14. Milshtein, J. D.; Kaur, A. P.; Casselman, M. D.; Kowalski, J. A.; Modekrutti, S.; Zhang, P. L.; Attanayake, N. H.; Elliott, C. F.; Parkin, S. R.; Risko, C.; Brushett, F. R.; Odom, S. A., High Current Density, Long Duration Cycling of Soluble Organic Active Species for Non-Aqueous Redox Flow Batteries. *Energy Environ. Sci.* **2016**, *9*, 3531-3543.
15. Li, S.; Ai, X.; Yang, H.; Cao, Y., A Polytriphenylamine-Modified Separator with Reversible Overcharge Protection for 3.6 V-Class Lithium-ion Battery. *J. Power Sources* **2009**, *189*, 771-774.
16. Pasala, V.; Ramachandra, C.; Sethuraman, S.; Ramanujam, K., A High Voltage Organic Redox Flow Battery with Redox Couples O₂/Tetrabutylammonium Complex and Tris (4-bromophenyl) amine as Redox Active Species. *J. Electrochem. Soc.* **2018**, *165*, A2696-A2702.
17. Dunn, R. P.; Kafle, J.; Krause, F. C.; Hwang, C.; Ratnakumar, B. V.; Smart, M. C.; Lucht, B. L., Electrochemical Analysis of Li-ion Cells Containing Triphenyl Phosphate. *J. Electrochem. Soc.* **2012**, *159*, A2100-A2108.
18. Casselman, M. D.; Kaur, A. P.; Narayana, K. A.; Elliott, C. F.; Risko, C.; Odom, S. A., The Fate of Phenothiazine-based Redox Shuttles in Lithium-ion Batteries. *Phys. Chem. Chem. Phys.* **2015**, *17*, 6905-6912.
19. Chen, Z.; Amine, K., Bifunctional Electrolyte Additive for Lithium-ion Batteries. *Electrochem. Commun.* **2007**, *9*, 703-707.
20. Zhang, L.; Zhang, Z.; Wu, H.; Amine, K., Novel Redox Shuttle Additive for High-Voltage Cathode Materials. *Energy Environ. Sci.* **2011**, *4*, 2858-2862.
21. Moshurchak, L.; Lamanna, W.; Bulinski, M.; Wang, R.; Garsuch, R. R.; Jiang, J.; Magnuson, D.; Triemert, M.; Dahn, J., High-Potential Redox Shuttle for Use in Lithium-ion Batteries. *J. Electrochem. Soc.* **2009**, *156*, A309-A312.
22. Bell, F.; Ledwith, A.; Sherrington, D., Cation-Radicals: tris-(p-Bromophenyl) Amminium perchlorate and hexachloroatimonate. *J. Chem. Soc. (C)* **1969**, 2719-2720.

- 1
2
3 23. Steckhan, E., Indirect Electroorganic Syntheses—A Modern Chapter of Organic
4 Electrochemistry [New Synthetic Methods (59)]. *Angew. Chem. Int. Ed. Engl* **1986**, *25*, 683-701.
5 24. Romero, N. A.; Nicewicz, D. A., Organic photoredox catalysis. *Chem. Rev.* **2016**, *116*,
6 10075-10166.
7 25. Christensen, J. A.; Phelan, B. T.; Chaudhuri, S.; Acharya, A.; Batista, V. S.; Wasielewski,
8 M. R., Phenothiazine radical cation excited states as super-oxidants for energy-demanding
9 reactions. *J. Am. Chem. Soc.* **2018**, *140*, 5290-5299.
10 26. Breslin, D. T.; Fox, M. A., Excited-state behavior of thermally stable radical ions. *J. Phys.*
11 *Chem.* **1994**, *98*, 408-411.
12 27. Grilj, J.; Laricheva, E. N.; Olivucci, M.; Vauthey, E., Fluorescence of radical ions in liquid
13 solution: wurster's blue as a case study. *Angew. Chem. Int. Ed.* **2011**, *50*, 4496-4498.
14 28. Green, S.; Fox, M. A., Intramolecular photoinduced electron transfer from nitroxyl
15 radicals. *J. Phys. Chem.* **1995**, *99*, 14752-14757.
16 29. Odom, S. A.; Ergun, S.; Poudel, P. P.; Parkin, S. R., A Fast, Inexpensive Method for
17 Predicting Overcharge Performance in Lithium-ion Batteries. *Energy Environ. Sci.* **2014**, *7*, 760-
18 767.
19 30. Mi, Z.; Yang, P.; Wang, R.; Unruangsri, J.; Yang, W.; Wang, C.; Guo, J., Stable Radical
20 Cation-Containing Covalent Organic Frameworks Exhibiting Remarkable Structure-Enhanced
21 Photothermal Conversion. *J. Am Chem. Soc.* **2019**, *141*, 14433-14442.
22 31. Fukui, N.; Cha, W.; Shimizu, D.; Oh, J.; Furukawa, K.; Yorimitsu, H.; Kim, D.; Osuka, A.,
23 Highly planar diarylamine-fused porphyrins and their remarkably stable radical cations. *Chem.*
24 *Sci.* **2017**, *8*, 189-199.
25 32. Maier, J.; Turner, D., Steric Inhibition of Resonance Studied by Molecular Photoelectron
26 Spectroscopy. Part 1.—Biphenyls. *Faraday Discuss. Chem. Soc.* **1972**, *54*, 149-167.
27 33. Andrews, L.; Arlinghaus, R. T.; Payne, C. K., Absorption Spectra of Substituted Biphenyl
28 and Related Cations in Solid Argon and a Comparison with Photoelectron Spectra. *J. Chem. Soc.*
29 *Faraday Transl. Mater. Res.* **1983**, *79*, 885-895.
30 34. Hutchison, G. R.; Ratner, M. A.; Marks, T. J., Hopping Transport in Conductive
31 Heterocyclic Oligomers: Reorganization Energies and Substituent Effects. *J. Am. Chem. Soc.*
32 **2005**, *127*, 2339-2350.
33 35. Zade, S. S.; Bendikov, M., Twisting of Conjugated Oligomers and Polymers: Case Study
34 of Oligo- and Polythiophene. *Chem. Eur. J.* **2007**, *13*, 3688-3700.
35 36. Pascal, R. A., Twisted acenes. *Chem. Rev.* **2006**, *106*, 4809-4819.
36 37. Casselman, M. D.; Elliott, C. F.; Modekrutti, S.; Zhang, P. L.; Parkin, S. R.; Risko, C.;
37 Odom, S. A., Beyond the Hammett Effect: Using Strain to Alter the Landscape of Electrochemical
38 Potentials. *Chemphyschem* **2017**, *18*, 2142-2146.
39 38. Ergun, S.; Casselman, M. D.; Kaur, A. P.; Attanayake, N. H.; Parkin, S. R.; Odom, S. A.,
40 Improved Synthesis of N-Ethyl-3, 7-Bis (Trifluoromethyl) Phenothiazine. *New J. Chem.* **2020**, *44*,
41 11349-11355.
42 39. Kaur, A. P.; Harris, O. C.; Attanayake, N. H.; Liang, Z.; Parkin, S. R.; Tang, M. H.; Odom,
43 S. A., Quantifying Environmental Effects on the Solution and Solid-State Stability of a
44 Phenothiazine Radical Cation. *Chem. Mater.* **2020**, *32*, 3007-3017.
45 40. Roth, H. D., Structure and Reactivity of Organic Radical Cations. In *Photoinduced*
46 *Electron Transfer IV*, Springer: 1992.
47 41. Schmittl, M.; Burghart, A., Understanding Reactivity Patterns of Radical Cations. *Angew.*
48 *Chem. Int. Ed. Engl.* **1997**, *36*, 2550-2589.
49
50
51
52
53
54
55
56
57
58
59
60

- 1
2
3
4 42. Connelly, N. G.; Geiger, W. E., Chemical Redox Agents for Organometallic Chemistry. *Chem. Rev.* **1996**, *96*, 877-910.
- 5
6 43. Talipov, M. R.; Rathore, R., Robust Aromatic Cation Radicals as Redox Tunable Oxidants. *Organic Redox Systems: Synthesis, Properties, and Applications* **2015**.
- 7
8 44. Talipov, M. R.; Hossain, M. M.; Boddeda, A.; Thakur, K.; Rathore, R., A Search for Blues
9 Brothers: X-ray Crystallographic/Spectroscopic Characterization of the Tetraarylbenzidine Cation
10 Radical as a Product of Aging of Solid Magic Blue. *Org. biomol. chem.* **2016**, *14*, 2961-2968.
- 11
12 45. Ebersson, L.; Larsson, B., Electron Transfer Reactions in Organic Chemistry. IX.*
13 Acyloxylation and/or Debromodimerization Instead of. *Acta Chem. Scand.* **1986**, *40*, 210-225.
- 14
15 46. Narayana, K. A.; Casselman, M. D.; Elliott, C. F.; Ergun, S.; Parkin, S. R.; Risko, C.;
16 Odom, S. A., N-Substituted Phenothiazine Derivatives: How the Stability of the Neutral and
17 Radical Cation Forms Affects Overcharge Performance in Lithium-ion Batteries. *ChemPhysChem*
2015, *16*, 1179-1189.
- 18
19 47. Ergun, S.; Elliott, C. F.; Kaur, A. P.; Parkin, S. R.; Odom, S. A., Controlling Oxidation
20 Potentials in Redox Shuttle Candidates for Lithium-ion Batteries. *J. Phys. Chem. C* **2014**, *118* (27),
21 14824-14832.
- 22
23 48. Bruker-AXS (2016). APEX3 Bruker-AXS Inc., Madison, WI, USA.
- 24
25 49. Krause, L.; Herbst-Irmer, R.; Sheldrick, G. M.; Stalke, D., Comparison of Silver and
26 Molybdenum Microfocus X-ray Sources for Single-Crystal Structure Determination. *J. Appl.*
Crystallogr. **2015**, *48*, 3-10.
- 27
28 50. Sheldrick, G. M., SHELXT–Integrated Space-Group and Crystal-Structure Determination.
Acta Crystallogr. A **2015**, *71*, 3-8.
- 29
30 51. Sheldrick, G. M., Crystal Structure Refinement with SHELXL. *Acta Crystallogr. C* **2015**,
71, 3-8.
- 31
32 52. Otwinowski, Z.; Minor, W., [20] Processing of X-ray Diffraction Data Collected in
33 Oscillation Mode. In *Methods Enzymol.*, Elsevier: 1997; Vol. 276, pp 307-326.
- 34
35 53. Frisch, M.; Trucks, G.; Schlegel, H.; Scuseria, G.; Robb, M.; Cheeseman, J.; Scalmani, G.;
36 Barone, V.; Mennucci, B.; Petersson, G., *Gaussian 09; Gaussian, Inc* **2009**, *32*, 5648-5652.
- 37
38 54. Compton, R. G.; Banks, C. E., *Understanding Voltammetry*. 2nd ed.; Imperial College
39 Press, London: 2011.
40
41
42
43
44
45
46
47
48
49
50
51
52
53
54
55
56
57
58
59
60

Table of Contents Image



Caption: Changes in adiabatic ionization potential and half wave oxidation potential with *ortho* and *para* substitution on an *N*-alkylated phenothiazine.